Cyclin D1 kinase activity is required for the self-renewal of mammary stem and progenitor cells that are targets of MMTV-ErbB2 tumorigenesis

Rinath Jeselsohn[1,*], **Nelson E. Brown**[1,*], **Lisa Arendt**[1,2], **Ina Klebba**[1,2], **Miaofen G. Hu**[1], **Charlotte Kuperwasser**[1,2,#], and **Philip W. Hinds**[1,#]

[1]Molecular Oncology Research Institute, Tufts Medical Center, Boston, MA 02111

[2]Department of Anatomy and Cellular Biology, Tufts University School of Medicine, Boston, MA 02111

Summary

Transplantation studies have demonstrated the existence of mammary progenitor cells with the ability to self-renew and regenerate a functional mammary gland. Although these progenitors are the likely targets for oncogenic transformation, correlating progenitor populations with certain oncogenic stimuli has been difficult. Cyclin D1 is required for lobuloalveolar development during pregnancy and lactation as well as MMTV-ErbB2- but not MMTV-Wnt1-mediated tumorigenesis. Using a kinase deficient cyclin D1 mouse, we identified two functional mammary progenitor cell populations, one of which is the target of MMTV-ErbB2. Moreover, cyclin D1 activity is required for the self-renewal and differentiation of mammary progenitors as its abrogation leads to a failure to maintain the mammary epithelial regenerative potential and also results in defects in luminal lineage differentiation.

Significance—The cellular origins of breast cancer-initiating cells have remained obscure. In addition, the heterogeneity of breast cancers into basal and luminal types based on protein and gene expression patterns suggests that different subtypes of breast cancers might arise from different target populations of breast epithelial cells. Identification of distinct stem or progenitor cell populations with different hormonal sensitivities and requirements for cyclin D1 activity is appealing as it implies that the cellular origins of certain types of breast cancer may have a similar specificity. These specific requirements among tumor subtypes may offer therapeutic targets in human breast tumors.

Keywords

Cyclin D1; lobule progenitors; cell fate; MMTV-ErbB2; tumor stem cells

#To whom correspondence may be addressed: Philip W. Hinds, Ph.D., Molecular Oncology Research Institute, Tufts Medical Center, 800 Washington Street, Box 5609, Boston, MA 02111, Phone: (617) 636-7947, Fax: (617) 636-7813, phinds@tuftsmedicalcenter.org, Charlotte Kuperwasser, Ph.D., Dept of Anatomy & Cell Biology, Tufts University School of Medicine, Molecular Oncology Research Institute, 800 Washington St, Box 5609, Boston, MA 02111, Phone: (617) 636-2364, Fax: (617) 636-6127, charlotte.kuperwasser@tufts.edu.
*These authors contributed equally to this work

Introduction

Breast cancer is a heterogeneous disease. Using gene expression profiling analysis, human breast cancers and mouse mammary tumor models have been broadly classified into either luminal-like or basal-like cancers (Perou et al., 2000). For example, the MMTV-Wnt1 tumor model has been shown to classify with human basal-like breast cancers, a fact very much in keeping with the observed association of Wnt signaling in human basal-like mammary tumors (DiMeo et al., 2009; Herschkowitz et al., 2007) while the MMTV-ErbB2 tumor model has been shown to classify with human luminal-type breast cancers (Herschkowitz et al., 2007). While it is presumed that these different tumor subtypes originate from different epithelial targets, the identity of these target cells is unclear.

The mammary gland is comprised of a heterogeneous population of cells ranging from terminally differentiated cells with limited proliferative potential to multipotent stem and progenitors cells with extensive proliferative, differentiative and self-renewal capacities. Two main epithelial cell types are found in the virgin mammary tissue: luminal cells that line the lumens and express hormone receptors, and myoepithelial cells which are localized at the interface between luminal cells and the basement membrane and have specialized contractile functions. A third secretory or alveolar cell type arises during pregnancy within the terminal ductal lobular units but undergo programmed cell death following the cessation of lactation.

An important and underappreciated feature of mammary tissues is the fact that they are composed of ducts and lobules, which are anatomically distinct structures with fundamentally different functions. Ducts are bifurcated linear structures that direct the flow of milk out of the gland whereas lobules are lateral side branching structures terminating in acinar pouchings that become alveoli during pregnancy. Consistent with this anatomical organization is the existence of multipotent progenitor cells that can be distinguished by their ability to produce lobule-limited, ductal-limited, or complete mammary outgrowths following transplantation (Kordon and Smith, 1998). All three cell types are thought to arise from a common precursor, but the precise cell types that generate ductal- or lobule-limited outgrowths have not been identified.

Several reports have described the identification of multipotent progenitor cells that exhibit self-renewal properties and can contribute to ductal, lobular, and alveolar morphogenesis (Booth et al., 2007). One type of stem/progenitor cell can be identified on the basis of a $CD24^{Med}CD29^{Hi}$ or $CD24^+CD49f^{Hi}$ cell surface phenotype (Shackleton et al., 2006; Stingl et al., 2006). However, a second type of progenitor cell has been reported that is capable of establishing a fully functional mammary gland upon transplantation at limiting dilution, and is able to generate all the diverse epithelial lineages present in the murine mammary tissue (Boulanger et al., 2005; Henry et al., 2004; Smith and Medina, 2008; Wagner et al., 2002). These progenitor cells, termed Parity-Identified Mammary Epithelial Cells (PI-MECs), are present in both nulliparous and parous glands, and can also give rise to lobule-limited structures (Smith and Medina, 2008). At present, the link between PI-MEC progenitor cells and $CD24^{Med}CD29^{Hi}$ or $CD24^+CD49f^{Hi}$ populations is unclear. In addition, it has been assumed that mammary stem/progenitor cells are the targets for oncogenic transformation, but identifying which progenitor population is the target for which oncogenic stimulus has been difficult.

Cyclin D1 is a critical component of the cell cycle that is required for mammary gland development. Cyclin D1 knockout mice fail to generate lobuloalveoli during pregnancy and cannot lactate (Fantl et al., 1995; Sicinski et al., 1995). Interestingly, cyclin D1 knockout mice are resistant to MMTV-ErbB2 mediated tumorigenesis, a fact very much in keeping with the observed overexpression of cyclin D1 in the majority of human luminal mammary tumors (Gauthier et al., 2007; Yu et al., 2001). In contrast, cyclin D1 knockout mice are still susceptible

to MMTV-Wnt1 mediated oncogenesis suggesting the possibility that these tumors originate from different epithelial targets that exhibit different sensitivities to cyclin D1 expression.

In order to dissect the roles of cyclin D1-associated kinase activity during mammary gland development and MMTV-ErbB2-induced tumorigenesis we have generated the point mutant cyclin D1 (K112E) knockin mouse. The cyclin D1-K112E protein can still bind to cyclin-dependent kinases 4 and 6 (Cdk4/6) but the resulting complexes are enzymatically inactive (Baker et al., 2005; Hinds et al., 1994). We have previously shown that cyclin D1$^{KE/KE}$ female mice displayed apparently developed lobuloalveoli following pregnancy, yet they remained protected against the development of MMTV-ErbB2-driven mammary tumors (Landis et al., 2006). In the current study, we sought to determine the cellular mechanisms by which the absence of cyclin D1-associated kinase activity does not seem to affect development but can block the formation of ErbB2-driven mammary tumors.

Results

PI-MEC progenitor cells are the targets of MMTV-ErbB2-mediated tumorigenesis and cannot be maintained in cyclin D1$^{KE/KE}$ mutant mice

We have previously reported that nulliparous mice deficient in cyclin D1 kinase activity failed to develop mammary tumors on a MMTV-ErbB2 background despite exhibiting normal lobuloalveolar development after a single round of pregnancy and lactation (Landis et al., 2006). However, it has been well established that the development of MMTV-ErbB2-driven mammary tumors can be accelerated following repeated cycles of pregnancy (Henry et al., 2004). Therefore, we first sought to determine whether multiple pregnancies in cyclin D1$^{KE/KE}$ mice might overcome their tumor resistance. We found that after three rounds of consecutive breeding cycles, cyclin D1$^{KE/KE}$/MMTV-ErbB2 mice remained resistant to the development of mammary tumors (Figure 1A). In contrast, cyclin D1$^{+/+}$/MMTV-ErbB2 mice exhibited accelerated mammary tumors as expected.

We next wanted to determine whether the inability of cyclin D1$^{KE/KE}$ mice to develop MMTV-ErbB2-driven tumors was due to a reduction in the number of the cellular targets for transformation. Recently, the cellular targets of MMTV-ErbB2-induced tumorigenesis have been suggested to reside within PI-MECs in parous animals (Boulanger et al., 2005; Henry et al., 2004; Smith and Medina, 2008; Wagner et al., 2002) as well as within a population of cells exhibiting a CD24$^+$Sca1$^+$ phenotype (Li et al., 2007; Liu et al., 2007). Therefore, we examined the number of CD24$^+$Sca1$^+$ cells as well as PI-MECs in cyclin D1$^{KE/KE}$ mice. FACS analysis performed on single-cell suspensions of mammary epithelium revealed a ~3-fold reduction in the number of CD24$^+$Sca1$^+$ progenitor cells and a ~2-fold increase in CD24^{Low} cells present in mammary glands of cyclin D1$^{KE/KE}$/MMTV-ErbB2 mice (Figure 1B). However, the fact that CD24$^+$Sca1$^+$ cells were still present in cyclin D1$^{KE/KE}$ mice suggested that this population might not be the cellular target for transformation.

We next assessed the number of PI-MECs in cyclin D1$^{KE/KE}$ mammary glands (Smith and Medina, 2008). Accordingly, we generated cyclin D1$^{KE/KE}$/MMTV-ErbB2/WAP-cre/Rosa-GFP mice in which the green fluorescent protein (GFP) is expressed following pregnancy-induced Cre-mediated recombination. As expected, the generation of GFP+ cells was confirmed during lactation in both cyclin D1$^{+/+}$ and cyclin D1$^{KE/KE}$ mice (Figure 1C, upper panels). Six weeks following post-lactational involution, we continued to detect a population of GFP+ cells in parous mammary glands of cyclin D1$^{+/+}$/MMTV-ErbB2/WAP-cre/Rosa-GFP mice consistent with the labeling of PI-MECs. In contrast, parous cyclin D1$^{KE/KE}$/MMTV-ErbB2/WAP-cre/Rosa-GFP mammary tissues retained very few GFP+ cells (Figure 1C, lower panels).

The near absence of PI-MECs in cyclin D1$^{KE/KE}$/MMTV-ErbB2 mice suggested that this population might contain the cell of origin for tumorigenesis in this model. Indeed, premalignant lesions originated in parous cyclin D1$^{+/+}$/MMTV-ErbB2/WAP-cre/Rosa-GFP mice were invariably GFP+, confirming that they were derived from PI-MECs (Figure 1D) (Henry et al., 2004). Collectively, these findings indicate that cyclin D1$^{KE/KE}$ mice are resistant to MMTV-ErbB2-induced tumorigenesis due to a lack of cellular targets of transformation, namely PI-MECs.

Cyclin D1 activity is required for mammary progenitor cell self-renewal and activity

The fact that virtually no PI-MECs were detectable in parous cyclin D1$^{KE/KE}$ mammary glands suggested a failure of this population to self-renew and, therefore, to be maintained following pregnancy. Consequently, we speculated that these mice might exhibit defects in the ability to form lobuloalveoli following successive cycles of pregnancy-induced proliferation and differentiation. Indeed, mammary tissues from cyclin D1$^{KE/KE}$ mice showed a pronounced failure to undergo full lobuloalveolar differentiation following a 3rd pregnancy (Figure 2A). This observation combined with the inability to maintain PI-MECs indicates that cyclin D1-associated kinase activity is necessary for the maintenance of progenitor cells.

To determine the extent to which other progenitor cell activities might also be compromised in the absence of cyclin D1 kinase activity, we examined the regenerative capacity of MECs isolated from mutant and wild-type mice following transplantation into cleared fat pads. Bi-potent stem cells give rise to two types of progenitor cells that mediate regenerative activities: ductal progenitors that give rise to cap cells and drive ductal elongation through the terminal end bud structure, and the lobule progenitors that produce the progeny for the side branches and lobular-alveolar development (Smith and Medina, 2008). Single-cell suspensions of cyclin D1$^{KE/KE}$ or cyclin D1$^{+/+}$ MECs were transplanted into contralateral cleared fat pads in a dilution series ranging from 50,000 to 2,000 cells. Both cyclin D1$^{+/+}$ and cyclin D1$^{KE/KE}$ MECs exhibited comparable engraftment rates at limiting dilutions and formed terminal end buds at the growing tips of the penetrating ducts 5 weeks after transplantation (Figure 2B and 2C, a). However, nearly 75% of all the outgrowths derived from cyclin D1$^{KE/KE}$ MECs failed to fill the entire fat pads while this only occurred in 35% of the transplants from cyclin D1$^{+/+}$ cells (Figure 2C, b. See also Table S1). In addition, there was a reduction in the overall number of ducts as well as a decrease in ductal size of mammary trees derived from cyclin D1$^{KE/KE}$ MECs (Figure 2C, b and c). Importantly, the ductal system derived from cyclin D1$^{KE/KE}$ MECs was nearly devoid of all side branching and lobules (Figure 2C, d–f and Figure S1). This observation was independent of the number of cells transplanted or the estrus status of the recipient mice at the time of sacrifice (see the Experimental Procedures). This finding indicates that mammary progenitor cell self-renewal is compromised in the absence of cyclin D1-associated kinase activity.

To further assess the defect in self-renewal activity, we examined the ability of cyclin D1$^{KE/KE}$ and cyclin D1$^{+/+}$ MECs to form spheres under non-adherent and serum free conditions (Dontu et al., 2003). We found that cyclin D1$^{+/+}$ and cyclin D1$^{KE/KE}$ MECs formed similar numbers of primary spheres (45±15.9 versus 36.7±8.7 for WT and KE, respectively, p=0.236. Figure 3A, left panels). However, secondary sphere formation was reduced ~2-fold in cyclin D1$^{KE/KE}$ MECs compared to cyclin D1$^{+/+}$ MECs (18.0±1.0 versus 36.7±7.1 for KE and WT cells, respectively, p=0.0212. Figure 3A, left panels) suggesting that the self-renewal capacity of progenitors was impaired in the absence of cyclin D1-associated kinase activity. We failed to observe any differences in the size of spheres between genotypes (Figure 3A left panels, and Figure 3A, a and b). Taken together, these data indicate that cyclin D1 activity is necessary for the regeneration of mammary tissues and the self-renewal of mammary progenitor cells. We also examined colony formation of sphere-derived cells in Matrigel. Colonies generated from

mutant spheres grew as spherical acinar structures that were smaller in size compared to those derived from cyclin D1$^{+/+}$ spheres (Figure 3A, c and d). In addition, confocal immunoflourescence microscopy analysis revealed that cyclin D1$^{KE/KE}$ acini were composed of an outer layer of SMA+ myoepithelial cells and an inner layer of luminal cells that failed to express E-cadherin (Figure 3A, e–f). This suggested that colony forming progenitor cells from cyclin D1$^{KE/KE}$ mammary glands lack full bi-potent activity compared to those derived from cyclin D1$^{+/+}$ mammary glands (see below). Taken together, these data indicate that cyclin D1 activity is necessary for regeneration of mammary tissues and for the self-renewal and differentiation of mammary progenitor cells.

Mammary tissues lacking cyclin D1 activity have reduced bi-potent CD24^{Hi}CD49f^{Low} cells

Since PI-MEC progenitors cannot be maintained in mammary glands of mice lacking cyclin D1 kinase activity, we reasoned that we could identify this population of cells by FACS, as it should be absent or greatly reduced in virgin cyclin D1$^{KE/KE}$ mice. Stem/progenitor cells with regenerative activity following transplantation into cleared fat pads can be enriched in either CD24^{Med}CD29^{Hi} or CD24^{Med}CD49f^{Hi} populations (Matulka et al., 2007; Shackleton et al., 2006; Stingl et al., 2006). Therefore, we first examined the distribution of CD24 and CD29 markers in cyclin D1$^{KE/KE}$ and cyclin D1$^{+/+}$ MECs preparations that were gated for CD45(−) cells. We found no significant difference in the number of CD24^{Med}CD29^{Hi} cells in cyclin D1$^{KE/KE}$ mammary glands compared to cyclin D1$^{+/+}$ tissues, suggesting that this population of progenitors was not affected by cyclin D1 activity (Figure S2A).

We next analyzed Lin(−) MECs from cyclin D1$^{KE/KE}$ mice using the cell surface markers CD24 and CD49f. Consistent with previous reports (Stingl et al., 2006), we identified two populations of cells in cyclin D1$^{+/+}$ as well as cyclin D1$^{KE/KE}$ mammary glands (Figure 3B). Non-committed progenitor cells are reported to reside within both CD24^{Med}CD49f^{Hi} and CD24^{Hi}CD49f^{Low} populations. CD24^{Med}CD49f^{Hi} cells enrich for mammary reconstitution units (MRU) that can regenerate an entire mammary tissue following transplantation, while CD24^{Hi}CD49f^{Low} cells enrich for colony forming cells (CFC) that can form heterogeneous colonies when plated *in vitro* (Stingl et al., 2006). Despite the reduced regenerative potential of cyclin D1$^{KE/KE}$ MECs, we found that mammary glands lacking cyclin D1 kinase activity contained increased numbers of CD24^{Med}CD49f^{Hi} cells as well as a significant decrease in CD24^{Hi}CD49f^{Low} cells (Figure 3B).

Since cells with the ability to form adherent colonies *in vitro* are enriched within the CD24^{Hi}CD49f^{Low} fraction (Stingl et al., 2001), and this population was reduced in cyclin D1$^{KE/KE}$ mammary tissues, we reasoned that the colony forming capacity of cyclin D1$^{KE/KE}$ MECs should be impaired. Indeed, we found that cyclin D1$^{KE/KE}$ MECs displayed decreased colony forming potential compared to cyclin D1$^{+/+}$ MECs (Figure 3C, left panels). In addition, when primary MECs are assayed in this way, they form three distinct luminal, myoepithelial and mixed colonies, derived from luminal, myoepithelial and bi-potent progenitors, respectively (Stingl et al., 2001). Luminal colonies consist of tightly arranged cuboidal cells while pure myoepithelial colonies have dispersed, teardrop-shaped cells. Mixed colonies are composed of a central core of tightly arranged cells surrounded by more dispersed cells. We observed that both cyclin D1$^{KE/KE}$ and cyclin D1$^{+/+}$ MECs were able to form all three types of colonies as confirmed by staining for alpha-smooth muscle actin (SMA), E-cadherin (E-cad) and cytokeratin 18 (CK18) (Figure 3C, a–c). However, cyclin D1$^{KE/KE}$ MECs formed fewer luminal colonies as well as greater numbers of myoepithelial colonies compared to MECs derived from cyclin D1$^{+/+}$ mammary tissues (Figure 3C, right panels). Consistent with this shift in cell fate in D1$^{KE/KE}$ MECs, we observed that cyclin D1 was expressed almost exclusively in luminal epithelial cells, but not in myoepithelial cells in these colonies (Figure S2B). These findings suggested that colony forming progenitor cells from cyclin D1$^{KE/KE}$

mammary glands lack full bi-potent activity compared to those from cyclin D1$^{+/+}$ mammary glands.

Mammary tissues contain distinct progenitor cell populations

The fact that cyclin D1$^{KE/KE}$ MECs are defective in progenitor cells with the ability to self-renew yet exhibit an increase in CD24^{Med}CD49f^{Hi} cells would seem conceptually inconsistent with the current mammary stem/progenitor cell model. Therefore, we first needed to exclude the possibility that CD24^{Med}CD49f^{Hi} cells might require cyclin D1 activity for proper function and differentiation. Accordingly, we examined the differentiation potential of sorted CD24^{Hi}CD49f^{Low} and CD24^{Med}CD49f^{Hi} cells from cyclin D1$^{KE/KE}$ and cyclin D1$^{+/+}$ mammary tissues. Progenitor cells within the CD24^{Hi}CD49f^{Low} population form spherical acinar structures, while CD24^{Med}CD49f^{Hi} cells form solid, irregular-shaped colonies when embedded in Matrigel (Stingl et al., 2006). Indeed, wild-type CD24^{Hi}CD49f^{Low} cells formed predominantly hollow spherical colonies, while CD24^{Med}CD49f^{Hi} cells formed predominantly solid spheres (Figure 4A). Importantly, we found that sorted CD24^{Hi}CD49f^{Low}cells from cyclin D1$^{KE/KE}$ mice displayed a marked decrease in the formation of large hollow acini compared to those derived from wild-type controls while the number and size of CD24^{Med}CD49f^{Hi}-derived colonies was indistinguishable between genotypes (Figure 4A and data not shown). In addition, we also examined the differentiation potential of Matrigel colonies for the presence of myoepithelial markers (cytokeratin 14 and SMA) and luminal epithelial markers (cytokeratin 18 and E-cadherin). CD24^{Med}CD49f^{Hi} MECs from cyclin D1$^{+/+}$ and cyclin D1$^{KE/KE}$ mammary tissues gave rise to similar numbers of colonies expressing the myoepithelial markers SMA or cytokeratin 14, or the luminal epithelial markers cytokeratin 18 or E-cadherin (Figure 4B, Figure S3A and data not shown). However, sorted CD24^{Hi}CD49f^{Low} cells from cyclin D1$^{KE/KE}$ tissues gave rise to a higher proportion of colonies containing SMA+ cells (Figure 4B) compared to sorted CD24^{Hi}CD49f^{Low} cells from cyclin D1$^{+/+}$ glands, suggesting a defect in the differentiation potential of this population in the absence of cyclin D1 kinase activity. To further confirm our findings, we assessed the mRNA expression levels of CD61, a reported marker for luminal progenitor cells (Asselin-Labat et al. 2007), in CD24/CD49f-sorted populations. We observed a significant 2-fold decrease in CD61 expression in CD24^{Hi}CD49f^{Low} MECs derived from cyclin D1$^{KE/KE}$ mammary glands compared to the same population derived from wild-type MECs (Figure S3B). However, there was no significant difference in CD61 expression between CD24^{Med}CD49f^{Hi} fractions from cyclin D1$^{KE/KE}$ and cyclin D1$^{+/+}$ MECs (Figure S3B). While these findings demonstrate that CD24^{Med}CD49f^{Hi} as well as CD24^{Hi}CD49f^{Low} populations both contain bi-potent progenitor cells, only CD24^{Hi}CD49f^{Low} cells exhibit defects in differentiation potential in the absence of cyclin D1 kinase activity.

Our findings suggest that a proportion of CD24^{Hi}CD49f^{Low} cells contain bi-potential progenitor activity, and this activity is impaired in the absence of cyclin D1 kinase activity. We therefore assessed the *in vivo* reconstitution activity of sorted CD24^{Med}CD49f^{Hi} and CD24^{Hi}CD49f^{Low} cells (5×10^4) derived from wild type mammary glands following transplantation into cleared mammary fat pads of either nulliparous (virgin) or pregnant hosts (Figure 4C). Consistent with previous studies, we found that sorted CD24^{Med}CD49f^{Hi} cells were indeed capable of ductal and lobular/alveolar development when transplanted into cleared fat pads of pregnant hosts, indicating that cells within this population have the capacity to undergo full lobuloalveolar differentiation under pregnancy-induced conditions (Stingl et al., 2006). However, we found that the ductal trees derived from CD24^{Med}CD49f^{Hi} MECs injected into nulliparous hosts were nearly devoid of all side branching and lobule development indicating that CD24^{Med}CD49f^{Hi} cells were unable to give rise to lobular/alveolar development in the absence of pregnancy (Figure 4C).

Moreover, we found that injection of CD24^{Hi}CD49f^{Low} cells not only generated ductal and lobular/alveolar outgrowths in pregnant hosts but also lobule-only and alveolar-only outgrowths (Figure 4C). Furthermore, we found that sorted CD24^{Hi}CD49f^{Low} cells produced ductal and lobular development with extensive side branching in nulliparous hosts indicating that bi-potent progenitor cells reside within this fraction and that these cells do not depend on the hormones of pregnancy for their differentiation potential (Figure 4C). It is worth noting that while CD24^{Med}CD49f^{Hi} and CD24^{Hi}CD49f^{Low} cells resulted in comparable engraftment rates and fat pad filling in the nulliparous host, sorted CD24^{Med}CD49f^{Hi} cells did exhibit a slight increase in fat pad filling in pregnant hosts, consistent with the notion that CD24^{Med}CD49f^{Hi} cells enrich for cells with greater mammary reconstituting activity in pregnant mice (Figure S3C) (Stingl et al., 2006).

Defects in luminal-lineage differentiation in the absence of cyclin D1 kinase activity

The data described above demonstrate a cyclin D1-activity dependence for the formation of lobular-alveolar structures, but also indicate that the ratio of luminal and myoepithelial cells is altered in cyclin D1$^{KE/KE}$ animals. To further explore this defect in epithelial differentiation, we stained cyclin D1$^{KE/KE}$ or cyclin D1$^{+/+}$ mammary tissues for markers of luminal (K18) and myoepithelial (SMA) differentiation. We found that myoepithelial cells within the main ducts of cyclin D1$^{KE/KE}$ and cyclin D1$^{+/+}$ mammary glands expressed SMA, but luminal cells in cyclin D1$^{KE/KE}$ glands lacked a robust K18 expression compared to cyclin D1$^{+/+}$ ducts (Figure 5A). In addition, while some reports suggest that keratin-6 (K6) is a marker of mammary progenitor cells, others have shown it to be abundantly expressed in differentiated luminal alveolar cells (Li et al., 2003; Smith et al., 1990). We found no K6 positive cells in cyclin D1$^{KE/KE}$ mammary tissues (data not shown). However, not all luminal markers were misexpressed, as the expression of estrogen (ERα) and progesterone receptors (PR-A and PR-B) was similar in luminal cells from both cyclin D1$^{KE/KE}$ and cyclin D1$^{+/+}$ glands (Figure 5A and data not shown). These data indicate that despite normal histological appearance, mammary ducts in cyclin D1$^{KE/KE}$ mice exhibit altered luminal cell differentiation.

Given these findings, we next examined ductal outgrowths from cyclin D1$^{+/+}$ and cyclin D1$^{KE/KE}$ transplants for evidence of perturbed luminal epithelial differentiation. Indeed, luminal cells of cyclin D1$^{KE/KE}$ ductal outgrowths did not express abundant E-cadherin and were negative for keratin-18 expression (Figure 5B). Furthermore, while K6 positive cells were found in the transplantation outgrowths derived from the cyclin D1$^{+/+}$ MECs, no K6 expression was detected in cyclin D1$^{KE/KE}$ outgrowths (Figure S4A). K6 positive cells in wild type ducts were localized to the inner layer of the ductal epithelium, were negative for SMA, and co-expressed GATA-3, the luminal marker and transcription factor required for luminal differentiation (Asselin-Labat et al., 2007; Kouros-Mehr et al., 2006). However, ductal outgrowths from cyclin D1$^{+/+}$ and cyclin D1$^{KE/KE}$ MECs both displayed a prominent outer layer of SMA positive, myoepithelial cells indicating that this lineage was not perturbed.

To further evaluate the defects in luminal cell differentiation, we analyzed dispersed single cell suspensions from cyclin D1$^{+/+}$ and cyclin D1$^{KE/KE}$ mammary tissues sorted by FACS. Differential staining of mammary epithelial cells on the basis of CD24 expression can discriminate between different lineages of mammary epithelial cells (Sleeman et al., 2006; Sleeman et al., 2007). Myoepithelial and luminal epithelial cells are identified as CD24^{Low} and CD24^{Hi}, respectively, while CD24 negative cells are considered to be non-epithelial cells. Using this approach, we found a significant increase in the percentage of CD24^{Low} (CD24L) cells and a significant reduction in the percentage of CD24^{Hi} (CD24H) cells in cyclin D1$^{KE/KE}$ MECs (Figure 5C, upper panels). To confirm that the disproportionate percentage of CD24L cells in cyclin D1$^{KE/KE}$ glands were myoepithelial cells, sorted CD24^{Low} and CD24^{Hi} cells were directly cytospun on glass slides and stained for SMA and E-cadherin. As

expected, most of the CD24L cells stained positive for SMA and negative for E-cadherin, while the majority of CD24H cells were E-cadherin positive and SMA negative (Figure 5C, lower panels, and Figure S4B). Next, gene expression patterns of CD24^{Hi} cells were examined using quantitative real-time PCR. We found that CD24^{Hi} luminal cells derived from cyclin D1$^{KE/KE}$ glands exhibit a reduction of CK18, GATA-3 and CK6 expression compared to cyclin D1$^{+/+}$ cells confirming that luminal cells exhibited altered differentiation in the absence of cyclin D1 kinase activity (Figure 5D). These findings imply that in the absence of cyclin D1-dependent kinase activity, differentiation of luminal cells is impaired and is accompanied by an accumulation of myoepithelial cells.

Discussion

Our results combined with those of others (Smith, 1996; Smith and Medina, 2008) support a more complex model of mammary gland hierarchy and differentiation. Multi-potent CD24$^+$CD49f$^+$ stem cells (PI-MECs) give rise to lineage-committed lobule progenitor cells (also termed PI-MECs in parous mice) and ductal progenitor cells, both of which have the capacity to give rise to luminal and myoepithelial cells, but exhibit different functional outgrowth potential (Figure 6). We found that PI-MECs require cyclin D1 kinase activity for their self-renewal as ductal and lobule outgrowth potential were significantly impaired following transplantation into clear fat pads. In addition, in mammary glands that could not maintain PI-MECs, luminal epithelial cell differentiation and tissue regeneration following serial rounds of pregnancy/lactation was also impaired. These data indicate that maintenance of PI-MECs and their progeny is necessary for long-term mammary tissue homeostasis and differentiation. Moreover, these data are consistent with previous reports, which have demonstrated that PI-MECs contain both multi-potent stem cells that self renew and generate diverse epithelial lineages of the murine mammary gland as well as lobule-committed progenitors (Boulanger et al., 2005; Henry et al., 2004; Smith and Medina, 2008; Wagner et al., 2002).

PI-MECs have also been reported to express both CD24 and CD49f surface markers (Boulanger et al., 2005; Henry et al., 2004; Smith and Medina, 2008; Wagner et al., 2002). Consistent with this notion, we observed that both CD24^{Hi}CD49f^{Low} and CD24^{Med}CD49f^{Hi} cells could regenerate complex mammary trees comprised of ducts, lobules and alveoli when transplanted into pregnant hosts. Remarkably, we found that while CD24^{Hi}CD49f^{Low} cells produced complex mammary outgrowths when implanted into cleared fat pads of nulliparous hosts, CD24^{Med}CD49f^{Hi} cells failed to develop ductal structures that contained side branches or lobules. This suggests that multi-potent stem cells are a minority subpopulation within CD24^{Med}CD49f^{Hi} cells that are only stimulated in the presence of pregnancy hormones. Therefore, it will be of great interest to identify additional markers beyond CD24 and CD49f that can further distinguish between multi-potent stem cells and lineage-committed progenitor cells.

It is worth noting that our findings are not inconsistent with previous reports, but rather extend the mammary hierarchy to incorporate the different functional lineages and anatomical structures that make up breast tissue. It is also worth noting that the transplant experiments described in this study were conducted in the presence of Matrigel. We did find that *in vivo* reconstitution activity of sorted CD24^{Hi}CD49f^{Low} cells was greatly compromised in the absence of Matrigel (data not shown). Consistent with this notion, co-injection with Matrigel in other stem cell assays has been reported to enhance engraftment of primary epithelial cells (Quintana et al., 2008). Consequently, the observations we have reported herein provide strong evidence that modification of the transplantation assay can enable the detection of progenitor cell activity and regeneration potential of mouse mammary epithelial cells. This has provided

for a means to identify additional stem/progenitor cell populations that appear to have diverse functional activities and exhibit unique sensitivity to pregnancy hormones.

In addition to expanding the mammary gland hierarchy, our data demonstrate that: (1) cyclin D1 activity is required for the maintenance of PI-MECs and lobule progenitor cells; (2) PI-MECs are the target of MMTV-ErbB2 mediated tumorigenesis and (3) the inability to maintain PI-MECs and lobule progenitor cells results in mammary tissues with a disproportionate number of myoepithelial cells and impaired state of differentiation of luminal epithelial cells.

Our data can also explain the described differential susceptibility of cyclin D1 knock out mice to different mammary oncogenes (Yu et al., 2001). Accordingly, MMTV-Wnt1 and MMTV-Myc driven tumors are likely to arise from ductal progenitor cells whereas MMTV-Ras and MMTV-ErbB2 tumors arise from lobule progenitor cells (Chepko et al., 2005; Shackleton et al., 2006). Recently, $CD29^{Hi}CD24^{Med}$ cells were found to expand in early hyperplastic lesions of MMTV-Wnt1 mammary glands but not in those transformed by MMTV-ErbB2 (Shackleton et al., 2006). It was proposed that this population of progenitor cells is likely to be the cellular origin of MMTV-Wnt1-driven transformation but not that of MMTV-ErbB2. As shown in our model (Figure 6), cyclin D1 kinase activity is required for the maintenance of lobule progenitors, the tumor initiating cells of MMTV-ErbB2 and MMTV-Ras mediated tumorigenesis, but is not required for the maintenance of the ductal progenitors, the tumor initiating cells of MMTV-Wnt1 and MMTV-Myc. In fact, we saw an increase in the $CD24^{Med}CD49f^{Hi}$ population that contains ductal progenitors in mammary glands lacking cyclin D1 activity, suggesting that loss of cyclin D1 could actually increase Wnt1- or Myc-induced tumorigenesis. In support of this possibility, cyclin D1 knockout mice that constitutively express beta-catenin in the mammary gland have an increased frequency and decreased latency for tumor development compared to MMTV-Wnt1 tumorigenesis (Rowlands et al., 2003).

Our initial finding that during a first pregnancy the cyclin $D1^{KE/KE}$ MECs are able to expand their lobuloalveolar units similarly to those of cyclin $D1^{+/+}$ MECs made it difficult to dissect the role of cyclin D1 as a regulator of development from that important for transformation. However, after successive pregnancies we observed a significant reduction in lobuloalveoli development similar to, but not as profound as the reduction seen the cyclin D1 knockout mouse after a first pregnancy. This delay in the developmental phenotype relative to that seen in the cyclin D1 knockout animals may indicate that a non-catalytic function of cyclin D1/Cdk complexes, such as titration of the cell cycle inhibitors $p27^{Kip1}$ and $p21^{Cip1}$, may be sufficient for the expansion of the ductal progenitors but only weakly able to influence lobule progenitor cell proliferation. The identity of the critical targets of these catalytic and noncatalytic functions of cyclin D1 in the mammary epithelium remains to be determined.

Although not as well studied, there is evidence to support the existence of a mammary epithelial hierarchy with bi-potent progenitors in the human breast (Stingl et al., 2001). Recently a unique population of cells which could be the human lobule progenitor has been identified. These cells are $EpCam^{Hi}CD49f^+$ (resembling the $CD24^{Hi}CD49f^+$ population in mice), exhibit increased colony-forming ability, and can give rise to both luminal and myoepithelial cells (Villadsen et al., 2007). Studying the effects of loss of cyclin D1 or CDK4 on this population could potentially help to understand the role of cyclin D1 in the human breast as well as further delineate the human mammary epithelial hierarchy.

Lastly, this study reiterates the importance of tailoring the treatment in breast cancer as well as other cancers to the biology of the tumor. As we show here, cyclin D1-associated kinase activity is critical for the maintenance of the cells driving MMTV-ErbB2 tumors as well as other luminal tumors but not for the cells driving tumors originating from ductal progenitor

cells. Our studies support the notion that treatments targeting cyclin D1 will be effective for the prevention and treatment of luminal type cancers but will most likely not be effective, and may even be deleterious to patients with basal type cancers.

Experimental Procedures

Mouse Strains

The generation of cyclin D1$^{KE/KE}$ mice was described previously (Landis et al., 2006). The MMTV–ErbB2 mouse (strain TG.NK) used in this study has been described elsewhere (Muller et al., 1988). ROSA26-GFP mice were purchased from the Jackson laboratories. WAP-cre transgenic mice were obtained from the NCI Mouse Models of Human Cancers Consortium. All animals used were treated humanely and in accordance with the Institutional Animal Care and Use committee at Tufts Medical Center approved protocols.

Preparation of single-cell suspensions

Mammary glands were harvested from 12-week old mice (except for PI-MECs studies in which mice were sacrificed 6 weeks post involution). Glands were mechanically disaggregated and then digested with collagenase (Sigma) and Hyaluronidase (Sigma) for 3–6 hours at 37°C. The resultant organoids were further digested in 0.25% trypsin-EDTA (2 min) and Dispase/DNAseI (5 min), and then filtered through a 40µm mesh. When necessary, Lin+ cells (Cd45+, CD31+ and Ter 119+) were immunomagnetically removed from freshly isolated cells using the Easysep mouse mammary stem cell enrichment kit (Stem Cell Technologies).

Mammary fat pad transplants

For limiting dilution experiments, freshly isolated MECs were resuspended in 40 µL of PBS and injected into cleared inguinal fat pads of 3-week old non-obese diabetic/severe combined immunodeficient (NOD/SCID) mice (Deome et al., 1959). Cyclin D1$^{KE/KE}$ or cyclin D1$^{+/+}$ MECs were transplanted into contralateral inguinal fat pads. Five weeks after transplantation glands were harvested and processed for whole mounting. Freshly sorted CD24^{Hi}CD49f^{Low} and CD24^{Med}CD49f^{Hi} cells purified from Balb/c mammary glands were resuspended in 25 µL of Matrigel:Medium (1:3) solution and injected into cleared inguinal fat pads of syngeneic Balb/c female mice. For nulliparous studies, 3-week old Balb/c females were used as hosts. For pregnant hosts, 3-week old Balb/c female mice were cleared of their endogenous epithelium and allowed to mature for 5 weeks. At 8 weeks, mice were mated and examined daily for positive plugs. Mice that were negative for plugs were used as age-matched nulliparous controls. Pregnant and non-pregnant control hosts were injected with sorted cells and three weeks after transplantation glands were harvested and processed for whole mounting. Before being sacrificed, the stage at the estrous cycle of each recipient mouse was determined by microscopic inspection of hematoxylin-stained vaginal smears. Transplantations were considered negative if there were no epithelial outgrowths, positive if the outgrowth appeared to originate from a central location and branch out in multiple directions. If the outgrowth appeared to originate from the side of the gland and the branching was mainly unidirectional the transplant was considered as a failed clearance. Percent filling was quantified under a dissecting microscope at 2× magnification using the following formula: % filling = length of ductal outgrowth/ total length of mammary fat pad.

Whole Mounts

Mammary glands were spread onto glass slides and fixed in glacial acetic acid:ethanol (1:3), hydrated and stained overnight in 0.2% carmine red. Glands were subsequently dehydrated with graded ethanol solutions, cleared in toluene and mounted.

Immunostaining

Tissue sections were incubated overnight at 4°C with primary antibodies diluted in 2% BSA/PBS. Secondary antibodies were applied for 1 hr at RT. Sections were counter-stained with DAPI whenever necessary. For cells cytospun directly onto glass slides, fixation was carried out in methanol:acetone (1:1) at −20°C for 10 minutes. A Nikon Eclipse 80t microscope and SPOT camera were used to analyze and photograph the stained sections. The antibodies used included SMA (Neomarkers), E-cadherin (Santa Cruz biotechnologies), CK18 (Abcam), K6 (Covance), GATA-3 (Santa Cruz Biotechnologies) and ERα (Dako).

Flow cytometry

Freshly isolated Lin(−) cells (CD45-, CD31- and Ter119-) were incubated with primary antibodies according to manufacture's instructions (Stem Cell Technology). Antibodies used were CD29 (Chemicon), CD24 and CD49f (Stem Cell Technology), CD45 (Caltag), and SCA-1 (BD Pharmingen). Cell sorting was carried out with a modular flow cytometer (Beckman-Coulter) and analysis was done with FlowJo.

In-vitro assays

Freshly isolated MECs (5×10^4) were seeded on 10cm plates containing subconfluent, gamma-irradiated NIH3T3 cells (5 Gy) as feeder layers. On day 5, mammary colonies were fixed with methanol, stained with crystal violet and counted. For sphere formation assays freshly isolated MECs (20,000 cells per 3ml) were plated on non-adherent plates (Corning) in serum-free medium. Primary spheres were dissociated with trypsin after 3 weeks and filtered through a 40µM mesh. Single cells were plated again in non-adherent plates for secondary spheres formation. When necessary, secondary spheres were also dissociated and single cells embedded in Matrigel (BD Biosciences) as described (Debnath et al., 2003). The resultant acini were fixed with 2% PFA on day 7 and stained as described (Debnath et al., 2003). Images were captured with a Leica TCS SP2 confocal microscope.

Quantitative RT-PCR

Total RNA from sorted cells was extracted using the RNeasy Mini Kit (Qiagen). cDNA was prepared using iScript kit (Biorad) and PCR was carried out with SYBR Green (Qiagen). The following primers were used in this study: CK18 Forward 5'-CTTGCTGGAGGATGGAGAAG-3' and CK18 Reverse 5'-CTGGCTGGAGCAGGAGATTCG-3'; GATA-3 Forward 5'-AGCCACATCTCTCCCTTCAG-3' and GATA-3 Reverse 5'-AGGGCTCTGCCTCTCTAACC-3'; CK6 Forward 5'-AGAGAGGGGTCGCATGAACT-3' and CK6 Reverse 5'-TCATCTGTTAGACTGTCTGCCTT-3'; CD61 Forward 5'-CCACACGAGGGGTGAACT-3' and CD61 Reverse 5'-CTTCAGGTTACATGGGGGTGA-3'. Samples were run on an Opticon2 detection system (MJ research). GAPDH was used as an internal control. Analysis was performed using the delta-delta ct method with the comparator being RNA extracted from wild-type unsorted cells.

Statistical Analysis

P-values were determined using a two-tailed distribution and two sample unequal variance Student's T-test.

Supplementary Material

Refer to Web version on PubMed Central for supplementary material.

Acknowledgments

References

Asselin-Labat ML, Sutherland KD, Barker H, Thomas R, Shackleton M, Forrest NC, Hartley L, Robb L, Grosveld FG, van der Wees J, et al. Gata-3 is an essential regulator of mammary-gland morphogenesis and luminal-cell differentiation. Nature cell biology 2007;9:201–209.

Baker GL, Landis MW, Hinds PW. Multiple functions of D-type cyclins can antagonize pRb-mediated suppression of proliferation. Cell cycle (Georgetown, Tex 2005;4:330–338.

Booth BW, Boulanger CA, Smith GH. Alveolar progenitor cells develop in mouse mammary glands independent of pregnancy and lactation. J Cell Physiol. 2007

Boulanger CA, Wagner KU, Smith GH. Parity-induced mouse mammary epithelial cells are pluripotent, self-renewing and sensitive to TGF-beta1 expression. Oncogene 2005;24:552–560. [PubMed: 15580303]

Chepko G, Slack R, Carbott D, Khan S, Steadman L, Dickson RB. Differential alteration of stem and other cell populations in ducts and lobules of TGFalpha and c-Myc transgenic mouse mammary epithelium. Tissue & cell 2005;37:393–412. [PubMed: 16137731]

Debnath J, Muthuswamy SK, Brugge JS. Morphogenesis and oncogenesis of MCF-10A mammary epithelial acini grown in three-dimensional basement membrane cultures. Methods (San Diego, Calif 2003;30:256–268.

Deome KB, Faulkin LJ Jr. Bern HA, Blair PB. Development of mammary tumors from hyperplastic alveolar nodules transplanted into gland-free mammary fat pads of female C3H mice. Cancer Res 1959;19:515–520. [PubMed: 13663040]

DiMeo TA, Anderson K, Phadke P, Fan C, Perou CM, Naber S, Kuperwasser C. A novel lung metastasis signature links Wnt signaling with cancer cell self-renewal and epithelial-mesenchymal transition in basal-like breast cancer. Cancer Res 2009;69:5364–5373. [PubMed: 19549913]

Dontu G, Abdallah WM, Foley JM, Jackson KW, Clarke MF, Kawamura MJ, Wicha MS. In vitro propagation and transcriptional profiling of human mammary stem/progenitor cells. Genes Dev 2003;17:1253–1270. [PubMed: 12756227]

Fantl V, Stamp G, Andrews A, Rosewell I, Dickson C. Mice lacking cyclin D1 are small and show defects in eye and mammary gland development. Genes Dev 1995;9:2364–2372. [PubMed: 7557388]

Gauthier ML, Berman HK, Miller C, Kozakeiwicz K, Chew K, Moore D, Rabban J, Chen YY, Kerlikowske K, Tlsty TD. Abrogated response to cellular stress identifies DCIS associated with subsequent tumor events and defines basal-like breast tumors. Cancer cell 2007;12:479–491. [PubMed: 17996651]

Henry MD, Triplett AA, Oh KB, Smith GH, Wagner KU. Parity-induced mammary epithelial cells facilitate tumorigenesis in MMTV-neu transgenic mice. Oncogene 2004;23:6980–6985. [PubMed: 15286714]

Herschkowitz JI, Simin K, Weigman VJ, Mikaelian I, Usary J, Hu Z, Rasmussen KE, Jones LP, Assefnia S, Chandrasekharan S, et al. Identification of conserved gene expression features between murine mammary carcinoma models and human breast tumors. Genome biology 2007;8:R76. [PubMed: 17493263]

Hinds PW, Dowdy SF, Eaton EN, Arnold A, Weinberg RA. Function of a human cyclin gene as an oncogene. Proc Natl Acad Sci U S A 1994;91:709–713. [PubMed: 8290586]

Kordon EC, Smith GH. An entire functional mammary gland may comprise the progeny from a single cell. Development (Cambridge, England) 1998;125:1921–1930.

Kouros-Mehr H, Slorach EM, Sternlicht MD, Werb Z. GATA-3 maintains the differentiation of the luminal cell fate in the mammary gland. Cell 2006;127:1041–1055. [PubMed: 17129787]

Landis MW, Pawlyk BS, Li T, Sicinski P, Hinds PW. Cyclin D1-dependent kinase activity in murine development and mammary tumorigenesis. Cancer cell 2006;9:13–22. [PubMed: 16413468]

Li Y, Welm B, Podsypanina K, Huang S, Chamorro M, Zhang X, Rowlands T, Egeblad M, Cowin P, Werb Z, et al. Evidence that transgenes encoding components of the Wnt signaling pathway preferentially induce mammary cancers from progenitor cells. Proc Natl Acad Sci U S A 2003;100:15853–15858. [PubMed: 14668450]

Li Z, Tognon CE, Godinho FJ, Yasaitis L, Hock H, Herschkowitz JI, Lannon CL, Cho E, Kim SJ, Bronson RT, et al. ETV6-NTRK3 fusion oncogene initiates breast cancer from committed mammary progenitors via activation of AP1 complex. Cancer cell 2007;12:542–558. [PubMed: 18068631]

Liu JC, Deng T, Lehal RS, Kim J, Zacksenhaus E. Identification of Tumorsphere- and Tumor-Initiating Cells in HER2/Neu-Induced Mammary Tumors. Cancer Res 2007;67:8671–8681. [PubMed: 17875707]

Matulka LA, Triplett AA, Wagner KU. Parity-induced mammary epithelial cells are multipotent and express cell surface markers associated with stem cells. Developmental biology 2007;303:29–44. [PubMed: 17222404]

Muller WJ, Sinn E, Pattengale PK, Wallace R, Leder P. Single-step induction of mammary adenocarcinoma in transgenic mice bearing the activated c-neu oncogene. Cell 1988;54:105–115. [PubMed: 2898299]

Perou CM, Sorlie T, Eisen MB, van de Rijn M, Jeffrey SS, Rees CA, Pollack JR, Ross DT, Johnsen H, Akslen LA, et al. Molecular portraits of human breast tumours. Nature 2000;406:747–752. [PubMed: 10963602]

Quintana E, Shackleton M, Sabel MS, Fullen DR, Johnson TM, Morrison SJ. Efficient tumour formation by single human melanoma cells. Nature 2008;456:593–598. [PubMed: 19052619]

Rowlands TM, Pechenkina IV, Hatsell SJ, Pestell RG, Cowin P. Dissecting the roles of beta-catenin and cyclin D1 during mammary development and neoplasia. Proc Natl Acad Sci U S A 2003;100:11400–11405. [PubMed: 13679587]

Shackleton M, Vaillant F, Simpson KJ, Stingl J, Smyth GK, Asselin-Labat ML, Wu L, Lindeman GJ, Visvader JE. Generation of a functional mammary gland from a single stem cell. Nature 2006;439:84–88. [PubMed: 16397499]

Sicinski P, Donaher JL, Parker SB, Li T, Fazeli A, Gardner H, Haslam SZ, Bronson RT, Elledge SJ, Weinberg RA. Cyclin D1 provides a link between development and oncogenesis in the retina and breast. Cell 1995;82:621–630. [PubMed: 7664341]

Sleeman KE, Kendrick H, Ashworth A, Isacke CM, Smalley MJ. CD24 staining of mouse mammary gland cells defines luminal epithelial, myoepithelial/basal and non-epithelial cells. Breast Cancer Res 2006;8:R7. [PubMed: 16417656]

Sleeman KE, Kendrick H, Robertson D, Isacke CM, Ashworth A, Smalley MJ. Dissociation of estrogen receptor expression and in vivo stem cell activity in the mammary gland. The Journal of cell biology 2007;176:19–26. [PubMed: 17190790]

Smith GH. Experimental mammary epithelial morphogenesis in an in vivo model: evidence for distinct cellular progenitors of the ductal and lobular phenotype. Breast cancer research and treatment 1996;39:21–31. [PubMed: 8738603]

Smith GH, Medina D. Re-evaluation of mammary stem cell biology based on in vivo transplantation. Breast Cancer Res 2008;10:203. [PubMed: 18304381]

Smith GH, Mehrel T, Roop DR. Differential keratin gene expression in developing, differentiating, preneoplastic, and neoplastic mouse mammary epithelium. Cell Growth Differ 1990;1:161–170. [PubMed: 1707299]

Stingl J, Eaves CJ, Zandieh I, Emerman JT. Characterization of bipotent mammary epithelial progenitor cells in normal adult human breast tissue. Breast cancer research and treatment 2001;67:93–109. [PubMed: 11519870]

Stingl J, Eirew P, Ricketson I, Shackleton M, Vaillant F, Choi D, Li HI, Eaves CJ. Purification and unique properties of mammary epithelial stem cells. Nature 2006;439:993–997. [PubMed: 16395311]

Villadsen R, Fridriksdottir AJ, Ronnov-Jessen L, Gudjonsson T, Rank F, LaBarge MA, Bissell MJ, Petersen OW. Evidence for a stem cell hierarchy in the adult human breast. The Journal of cell biology 2007;177:87–101. [PubMed: 17420292]

Wagner KU, Boulanger CA, Henry MD, Sgagias M, Hennighausen L, Smith GH. An adjunct mammary epithelial cell population in parous females: its role in functional adaptation and tissue renewal. Development (Cambridge, England) 2002;129:1377–1386.

Yu Q, Geng Y, Sicinski P. Specific protection against breast cancers by cyclin D1 ablation. Nature 2001;411:1017–1021. [PubMed: 11429595]
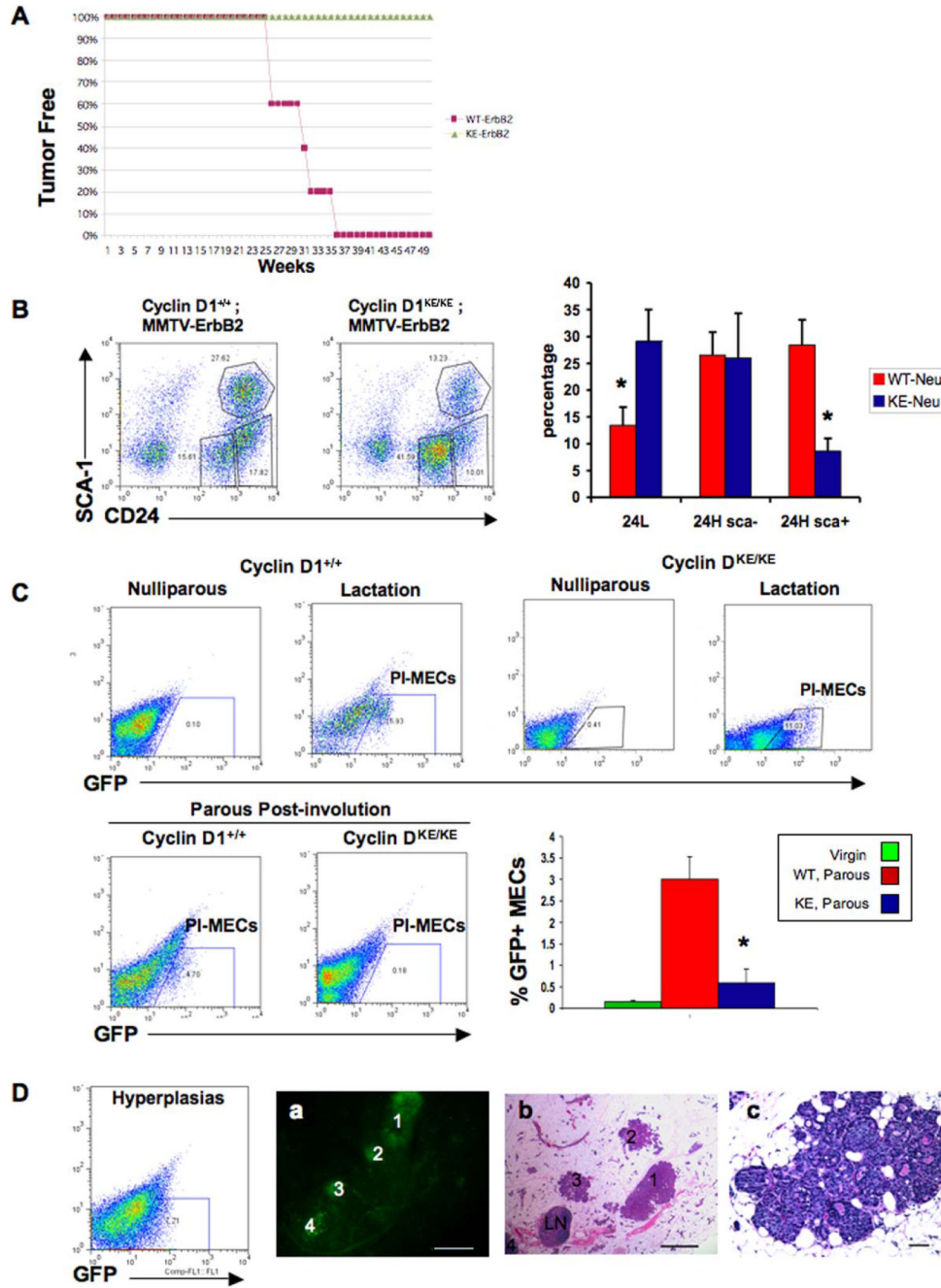
Figure 1. PI-MECs are reduced in cyclin D1KE/KE mice and are the targets of MMTV-ErbB2-mediated transformation

(A) Tumor-free curve of multiparous (three rounds of pregnancy and involution) cyclin D1+/+/MMTV-ErbB2 and cyclin D1KE/KE/MMTV-ErbB2 females.

(B) Flow cytometry analysis for CD24 and Sca surface markers showing a decrease in the CD24+Sca1+ population (24H, Sca+) in cyclin D1KE/KE/MMTV-ErbB2 MECs compared to cyclin D1+/+/MMTV-ErbB2 littermates. Error bars indicate mean ± SD. (*) indicates p value < 0.001.

(C) **Upper panels**. Flow cytometry analysis for the detection of GFP positive cells in virgin and lactating cyclin D1+/+/MMTV-ErbB2/Wap-Cre/Rosa-GFP mammary glands (cyclin

D1$^{+/+}$: Nulliparous, Lactation) as well as virgin and lactating cyclin D1$^{KE/KE}$ /MMTV-ErbB2/ Wap-Cre/Rosa-GFP (cyclin D1$^{KE/KE}$: Nulliparous, Lactation). **Lower panels and graph**. Flow cytometry analysis showing GFP positive cells (PI-MECs) derived from cyclin D1$^{+/+}$/ MMTV-ErbB2/Wap-Cre/Rosa-GFP (cyclin D1$^{+/+}$) and cyclin D1$^{KE/KE}$/MMTV-ErbB2/Wap-Cre/ Rosa-GFP (cyclin D1$^{KE/KE}$) mammary glands six weeks post-lactational involution. Error bars indicate mean $\pm$ SD. (*) indicates p value < 0.001.

(D) The expansion of the GFP positive cells was detected by flow cytometry analysis performed on MECs derived from a parous non-pregnant cyclin D1$^{+/+}$/MMTV-ErbB2/Wap-Cre/Rosa-GFP mammary gland with early hyperplastic lesions (hyperplasias). (a) A freshly isolated mammary gland from a parous non-pregnant cyclin D1$^{+/+}$/MMTV-ErbB2/Wap-Cre/Rosa-GFP mouse revealing GFP positive lesions (numbered 1 to 4) under fluorescence microscopy. Scale bar, 100µm. (b) Hemotoxylin and eosin (H&E)-stained section from the same mammary gland in (a) showing that GFP positive lesions represent early hyperplastic lesions. The lymph node (LN) is GFP negative. Scale bar, 100µm. (c) Higher magnification of a hyperplastic lesion. Scale bar, 50µm.
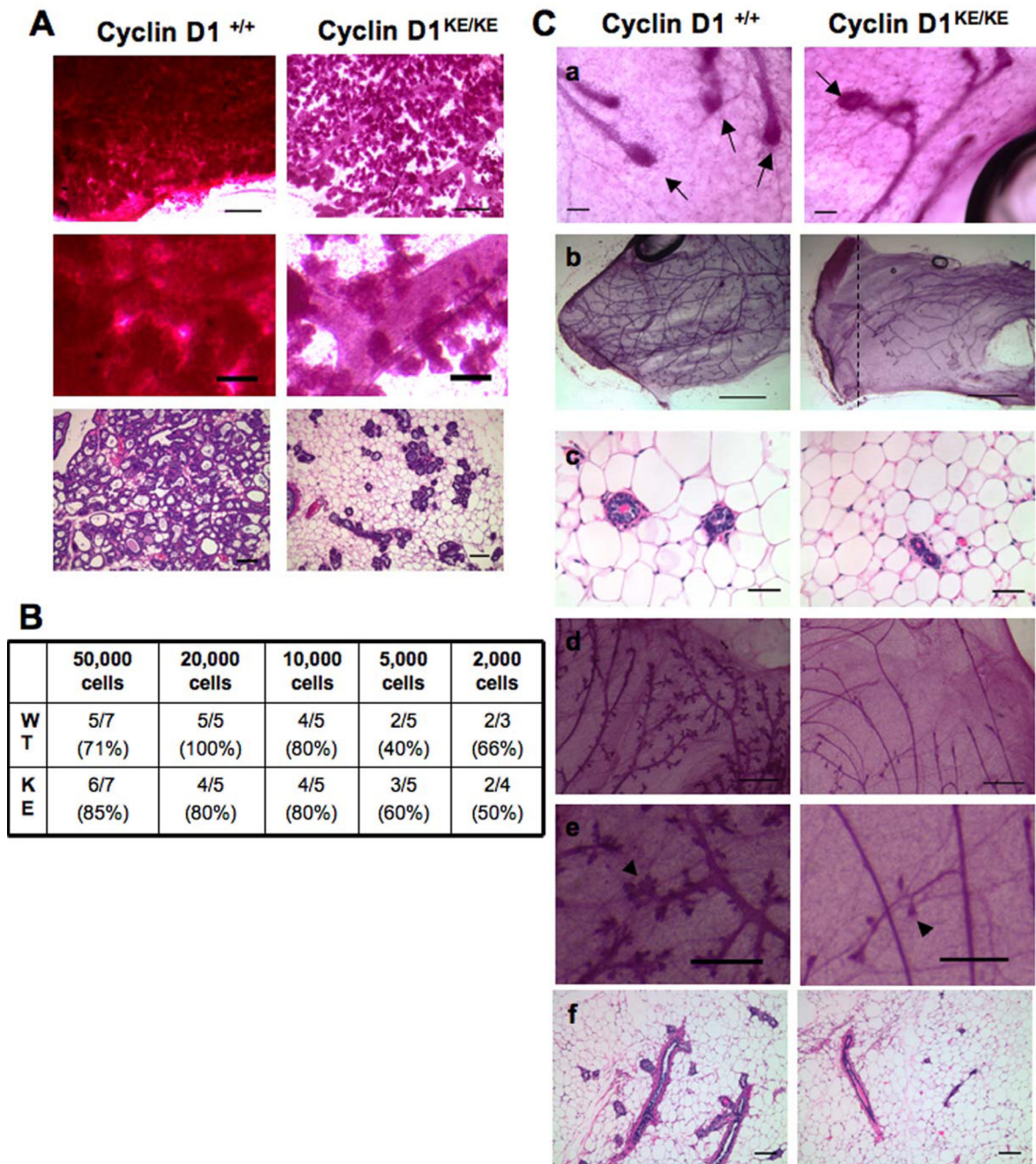
Figure 2. Cyclin D1 kinase activity is required for the maintenance and activity of progenitor cells in the mammary gland

(A) Mammary glands obtained from multiparous (three rounds of pregnancy and involution) cyclin D1^{+/+} and cyclin D1[KE/KE] mice were morphologically analyzed one day post-partum. Whole mounts and H&E-stained sections are shown. Notice the failure to undergo normal lobuloalveolar expansion observed in cyclin D1[KE/KE] mammary tissue. Middle panels represent a higher magnification of top panels. Scale bars: top, 100µm; middle, 25µm; and lower, 100µm.

(B) Overview of dilutional transplantation experiments showing that cyclin D1$^{+/+}$ and cyclin D1$^{KE/KE}$ MECs have similar engrafting capacity. The number of successful transplants per total injections is indicated.

(C) Ductal outgrowths derived from transplantation of cyclin D1$^{KE/KE}$ MECs have normal terminal end buds (a). Scale bar, 100µm. Arrows indicate terminal end buds. (b) Cyclin D1$^{KE/KE}$ ductal outgrowths fail to reach the end of the fat pad. Scale bar, 200µm. (c) Decrease in the size of the ducts derived from cyclin D1$^{KE/KE}$ MECs transplants as seen in H&E staining. Scale bar, 40µm. (d–f) Profound reduction in the side branching and lobules of outgrowths derived from cyclin D1$^{KE/KE}$ MECs. Whole mount analysis (d) and H&E staining (f) are shown. Middle panels represent a higher magnification of top panels. Scale bars: (d), 100µm; (e), 50µm; (f), 100µm. See also Table S1 and Figure S1.
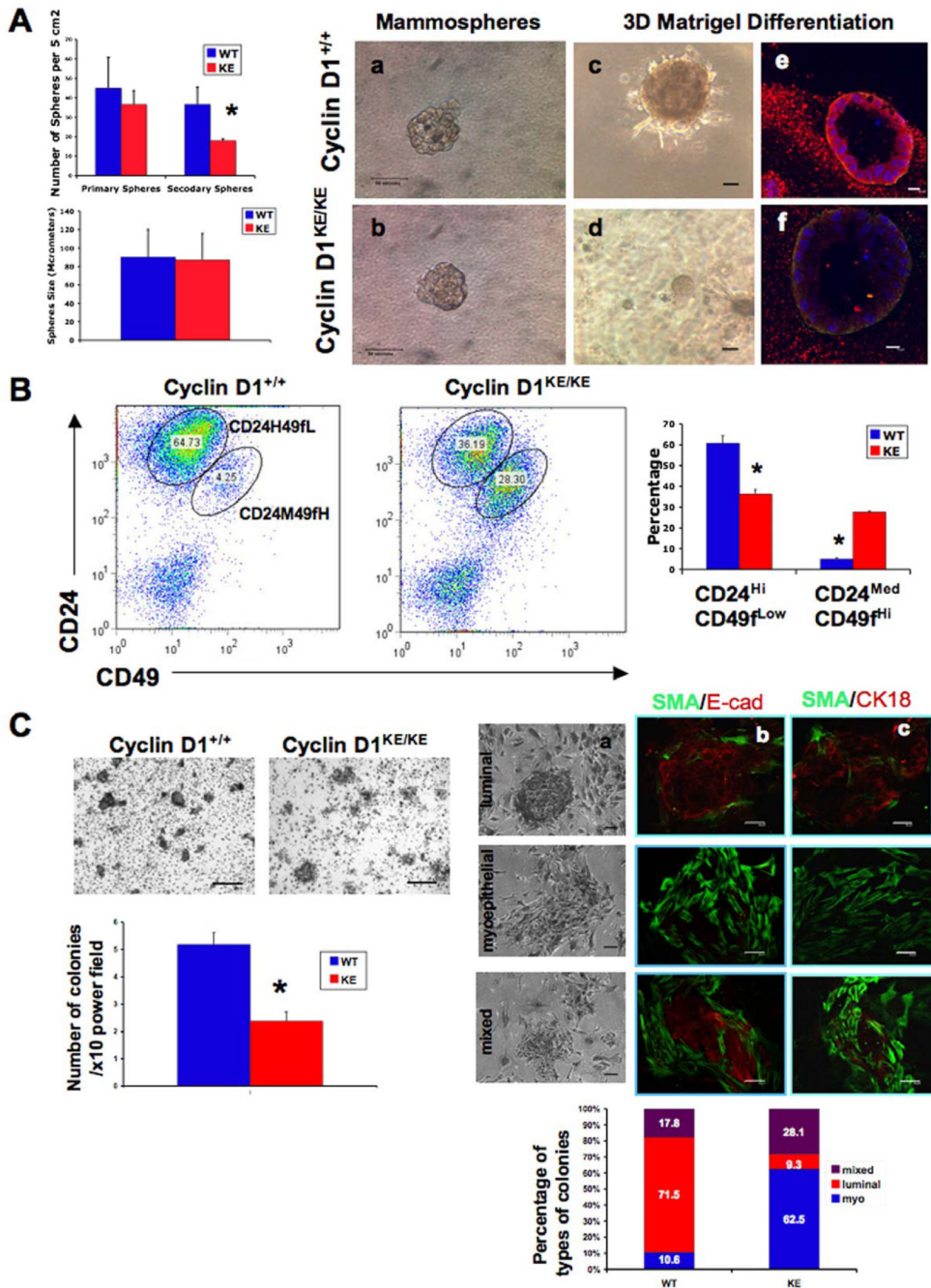
Figure 3. Lack of cylin D1 kinase activity leads to decreased selfrenewal of mammary progenitors and a reduction in the CD24^{Hi}CD49f^{Low} population

(A) **Left panels**. Sphere formation assays for cyclin D1$^{+/+}$ and cyclin D1$^{KE/KE}$ MECs plated in low-attachment plates and serum-free conditions (see Experimental Procedures). Quantification of the number of primary and secondary spheres per 5cm^2 and the size of secondary mammospheres (in μm) is shown. There was no significant difference in the number of primary spheres formed by cyclin D1$^{+/+}$ and cyclin D1$^{KE/KE}$ MECs (p=0.236). The number of secondary spheres, however, was significantly reduced in the context of KE mutation (p value < 0.05). The size of secondary spheres was similar between genotypes. Error bars indicate mean ± SD. (*) indicates p value < 0.05. **Right panels**. Secondary spheres derived from cyclin

D1$^{+/+}$ and cyclin D1$^{KE/KE}$ MECs (a,b) were dissociated on day 21 and embedded in Matrigel (c,d). The resulting acinar structures were stained for DAPI (blue), smooth muscle actin (green) and E-cadherin (red) and analyzed by confocal microscopy (e,f). Scale bars: (a–d), 50µm; (e,f), 10µm.

(B) Flow cytometry analysis showing the distribution of Lin(−) MECs for the expression of the surface markers CD24 and CD49f. Notice the decrease in the CD24^{Hi}CD49f^{Low} and the increase in the CD24^{Med}CD49f^{Hi} cell fractions in cyclin D1$^{KE/KE}$ MECs compared to cyclin D1$^{+/+}$ MECs. Error bars indicate mean ± SD. (*) indicates p value < 0.01.

(C) **Left panels**. Crystal violet staining of epithelial colonies formed on a feeder layer of growth-arrested fibroblasts (see Experimental Procedures). Quantification of the number of colonies per 10× field is shown. Notice the reduction in the number of colonies generated by cyclin D1$^{KE/KE}$ MECs. Error bars indicate mean ± SD. (*) indicates p value <0.001. **Right panels**. Three distinct types of colonies (luminal, myoepithelial, and mixed) were identified based on both morphology (a) and immunostaining (b and c). A quantification of the proportions of the different types of colonies derived from cyclin D1$^{+/+}$ and cyclin D1$^{KE/KE}$ MECs is shown. SMA, smooth muscle actin; E-cad, E-cadherin; CK18, cytokeratin 18. Scale bars: (a), 20µm; (b,c), 50µm. See also Figure S2.
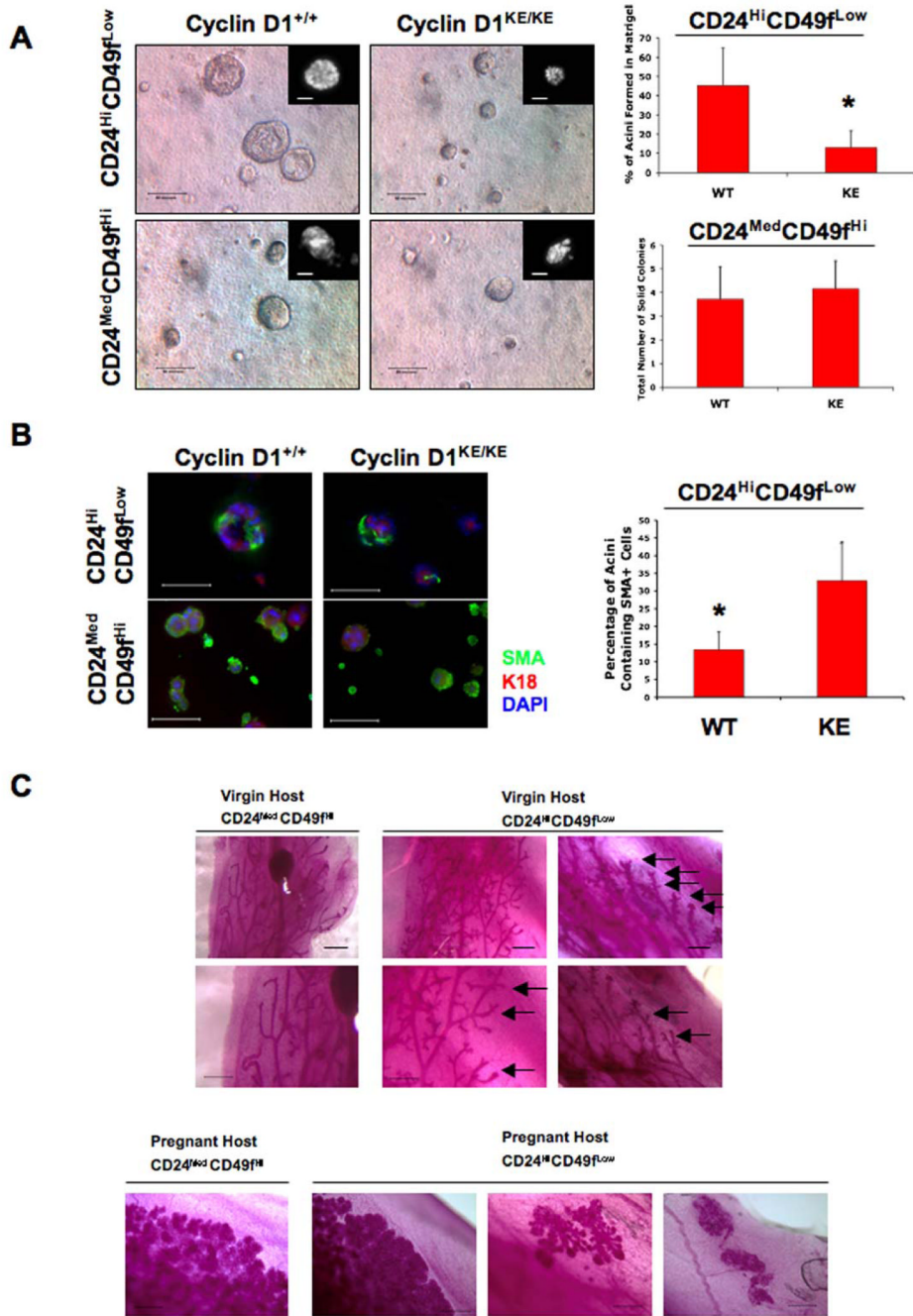
Figure 4. Mammary tissues lacking cyclin D1 kinase activity have reduced bi-potent CD24^{Hi}CD49f^{Low} cells

(A) CD24^{Hi}CD49f^{Low} and CD24^{Med}CD49f^{Hi} populations derived from cyclin D1$^{+/+}$ and cyclin D1$^{KE/KE}$ MECs were embedded in Matrigel (Debnath et al., 2003) and the type and number of colonies formed was microscopically assessed 10 days later. As expected, CD24^{Hi}CD49f^{Low} cells derived from cyclin D1$^{+/+}$ MECs gave rise to large lumen-containing structures (acini). However, the number of acini formed by CD24^{Hi}CD49f^{Low} cells was dramatically reduced in the context of cyclin D1 kinase activity deficiency. No significant difference was observed in the number and size of solid colonies generated from

CD24^{Med}CD49f^{Hi} populations of either genotype. Insets show DAPI-stained representative colonies. Scale bar, 50µm. Error bars indicate mean ± SD. (*) indicates p value <0.01.

(B) Colonies generated in (A) were subjected to immunofluorescence for the detection of myoepithelial (SMA) and luminal epithelial cell (K18) markers. Most acini generated from wild type CD24^{Hi}CD49f^{Low} cells were negative for SMA. However, ~12% of them showed the presence of SMA positive cells. This proportion was increased to ~30% in colonies generated from mutant CD24^{Hi}CD49f^{Low} cells. On the other hand, most structures generated from CD24^{Med}CD49f^{Hi} cells were strongly positive for SMA (>90%), with ~20% of them showing strong K18 co-staining. No differences in staining between genotypes were observed in this fraction of cells. SMA, smooth muscle actin; K18, keratin-18. Scale bar, 50µm. Error bars indicate mean ± SD. (*) indicates p value <0.001. See also Figures S3A and S3B.

(C) **Upper panels**. Whole mounts of outgrowths derived from sorted CD24^{Med}CD49f^{Hi} and CD24^{Hi}CD49f^{Low} populations purified from wild type nulliparous mice. 5×10^4 CD24^{Med}CD49f^{Hi} or 5×10^4 CD24^{Hi}CD49f^{Low} cells were injected into cleared fat pads of virgin Balb/c female mice. Representative ductal trees illustrate the duct-only derived growths from sorted CD24^{Med}CD49f^{Hi} cells while CD24^{Hi}CD49f^{Low} cells gave rise to ducts and lobules under the same conditions. Arrows: lobule side branches. **Lower Panels**. Lobular/alveolar outgrowths derived from sorted CD24^{Med}CD49f^{Hi} and CD24^{Hi}CD49f^{Low} cells transplanted into cleared fat pads of pregnant hosts. 5×10^4 CD24^{Med}CD49f^{Hi} or 5×10^4 CD24^{Hi}CD49f^{Low} cells were injected into cleared fat pads of pregnant Balb/c female mice. Representative whole mounts of ductal/alveolar trees illustrating the lobular/alveolar growths derived from sorted CD24^{Med}CD49f^{Hi} and CD24^{Hi}CD49f^{Low} cells are shown. Note that CD24^{Hi}CD49f^{Low} cells also produced lobule-only and acinar-only growths in pregnant hosts. Scale bars, 500µm. See also Figure S3C.
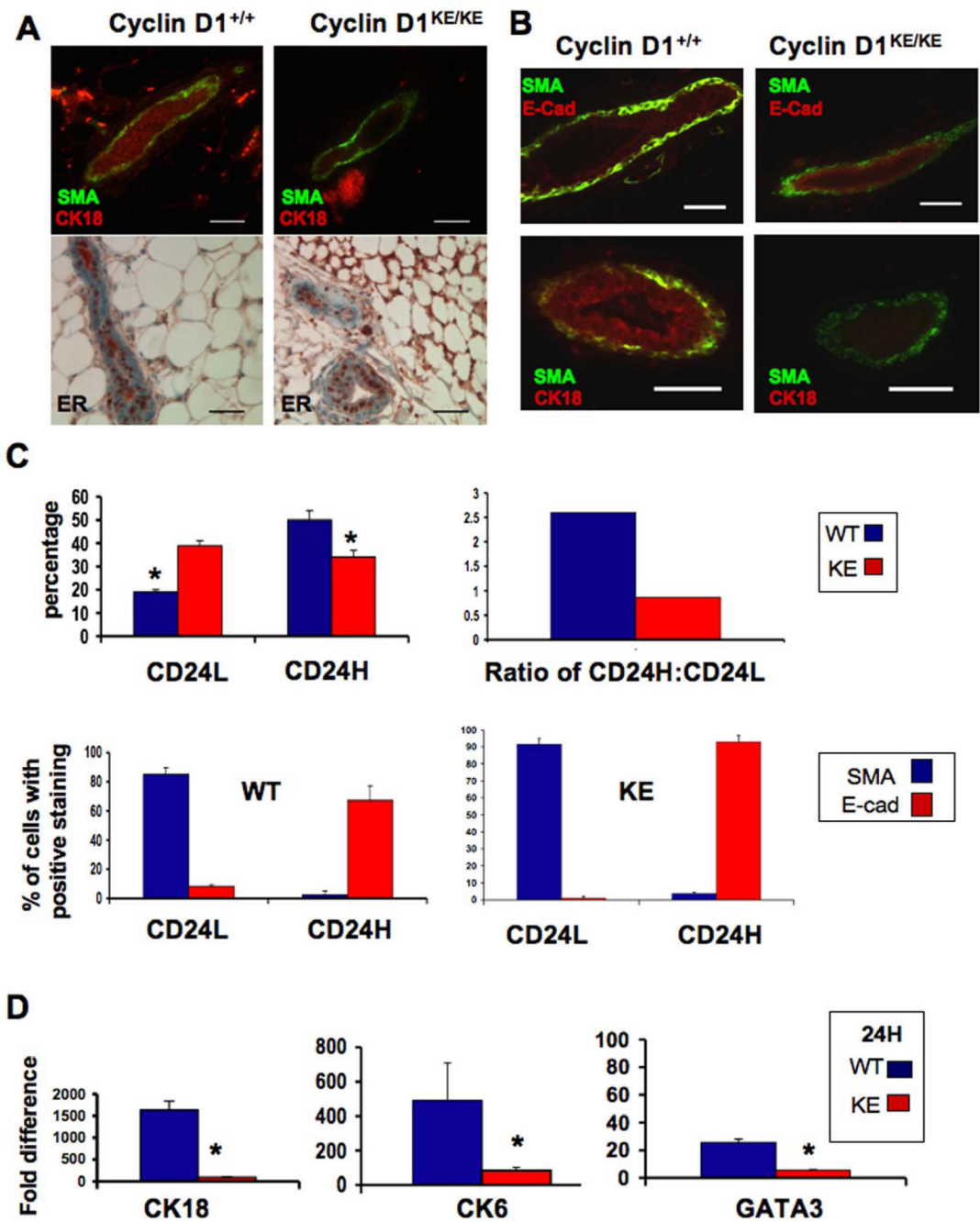
Figure 5. Defects in luminal-lineage differentiation in the absence of cyclin D1 kinase activity
(A) Immunofluorescence and immunohistochemical analysis of innate mammary glands derived from cyclin D1+/+ and cyclin D1KE/KE mice. Co-stainings for SMA (green) and CK18 (red) and stainings for estrogen receptor alpha (ER) are shown. Notice the reduced CK18 staining in cyclin D1KE/KE tissue compared to its cyclin D1+/+ counterpart. No difference in ER staining was observed. SMA, smooth muscle actin; CK18, cytokeratin-18; ER, estrogen receptor. Scale bar, 40µm.
(B) Immunofluorescense staining of ducts derived from transplants of cyclin D1+/+ and cyclin D1KE/KE MECs for the myoepithelial marker SMA (green) and luminal markers E-cadherin

or CK18 (red). SMA, smooth muscle actin; CK18, cytokeratin-18; E-Cad, E-cadherin. Scale bar, 40µm. See also Figure S4A.

(C) **Upper panels**. Cyclin D1$^{+/+}$ and cyclin D1$^{KE/KE}$ MECs were analyzed by flow cytometry for the expression of the surface marker CD24. There was an increase in the CD24^{Low} population (CD24L) and a reduction in the CD24^{Hi} population (CD24H) in cyclin D1$^{KE/KE}$ MECs (KE) compared to cyclin D1$^{+/+}$ MECs (WT). The CD24H : CD24L ratio for each genotype is also shown. (*) indicates p value <0.05. **Lower panels**: CD24-sorted cells were cytospun directly on glass slides and subsequently stained by for SMA and E-cadherin. As expected, the majority of CD24^{Hi} cells (CD24H) were E-cadherin positive and SMA negative and the opposite was observed for CD24^{Low} populations (CD24L). SMA, smooth muscle actin; E-Cad, E-cadherin. Error bars indicate mean ± SD. See also Figure S4B.

(D) Gene expression analysis of CD24^{Hi} populations for CK18, CK6 and GATA3 by quantitative RT-PCR. Error bars indicate mean ± SD. (*) indicates p value < 0.01.
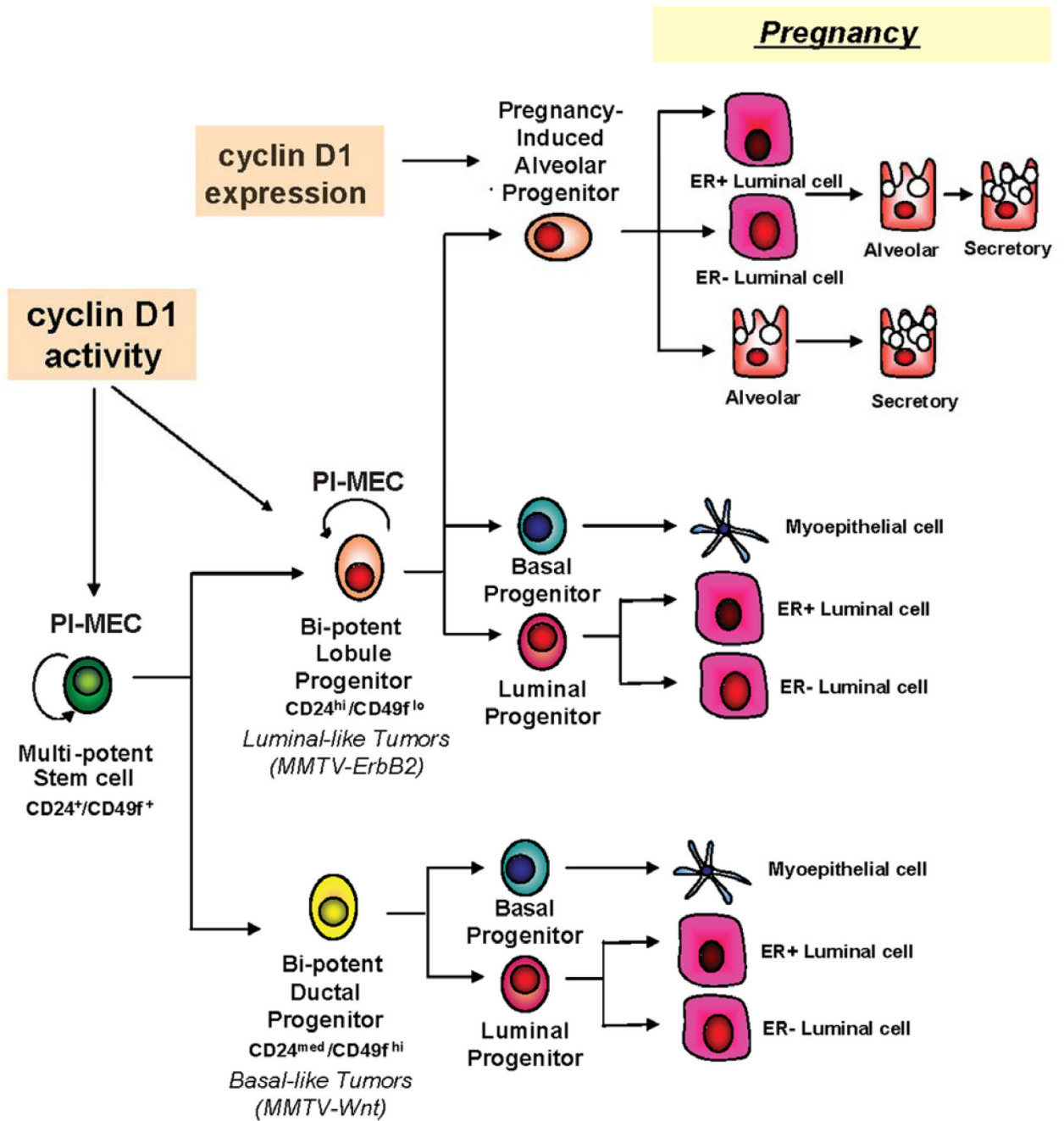
Figure 6. The role of cyclin D1 in the mammary epithelial hierarchy
A proposed model of the mammary epithelial cell developmental hierarchy in which cyclin D1 expression and activity are required for the maintenance of the lobule progenitors which are synonymous with the PI-MEC population.